Published in final edited form as:
J Neurol Neurosurg Psychiatry. 2012 July ; 83(7): 681–686. doi:10.1136/jnnp-2011-301969.

Fluorodeoxyglucose positron emission tomography in anti-N-methyl-D-aspartate receptor encephalitis: distinct pattern of disease

Frank Leypoldt[1], **Ralph Buchert**[2], **Ingo Kleiter**[3], **Jörg Marienhagen**[4], **Mathias Gelderblom**[1], **Tim Magnus**[1], **Josep Dalmau**[5], **Christian Gerloff**[1], and **Jan Lewerenz**[6]

[1]Department of Neurology, University Medical Center Eppendorf, Hamburg, Germany

[2]Department of Nuclear Medicine, Charité, Berlin, Germany

[3]Department of Neurology, St Josef-Hospital, Ruhr University Bochum, Bochum, Germany

[4]Department of Nuclear Medicine, University Medical Center Regensburg, Regensburg, Germany

[5]Department of Neurology, IDIBAPS/Hospital Clinic, University of Barcelona, Barcelona, Spain

[6]Department of Neurology, University Hospital Ulm, Ulm, Germany

Abstract

Background—Patients with encephalitis associated with antibodies against N-methyl-D-aspartate-receptor antibody (NMDAR-ab) encephalitis frequently show psychotic symptoms, amnesia, seizures and movement disorders. While brain MRI in NMDAR-ab encephalitis is often normal, abnormalities of cerebral glucose metabolism have been demonstrated by positron emission tomography (PET) with 18F-fluorodeoxyglucose (FDG) in a few usually isolated case reports. However, a common pattern of FDG-PET abnormalities has not been reported.

Methods—The authors retrospectively identified six patients with NMDAR-ab encephalitis in two large German centres who underwent at least one whole-body FDG-PET for tumour screening between January 2007 and July 2010. They analysed the pattern of cerebral uptake derived from

Correspondence to: Dr Frank Leypoldt, Department of Neurology, University Medical Center Eppendorf, Martinistr 52, Hamburg 20246, Germany; f.leypoldt@uke.uni-hamburg.de; Dr Jan Lewerenz, Department of Neurology, Oberer Eselsberg 45, 89081 Ulm, Germany; jan.lewerenz@uni-ulm.de.
FL and RB contributed equally to the manuscript.

Contributors: FL, IK, JM, MG, JL: study design. JM: patient selection. FL, IK, JL: data analysis. FL, RB, IK, JL: data interpretation. RB: statistical analysis. FL, RB, MG, TM, JD, CG, JL: drafting of the manuscript. IK, CG: revision of the manuscript.

Patient consent: Standardised patient consent forms were signed by all patients and controls.

Ethics approval: This is a retrospective case series. Written permission was obtained from all patients and controls. Therefore, no Ethics Committee approval was obtained.

Provenance and peer review: Not commissioned; externally peer reviewed.

Competing interests: FL received honoraria from Abbot and Talecris and research support from the Werner-Otto-Stiftung. IK received speaker honoraria and travel reimbursements from Bayer Healthcare, Biogen Idec, Merck Serono and Novartis, and research funding from Bayer Healthcare and Deutsche Forschungsgesellschaft. JM received honoraria from PETNet, Erlangen, Germany and research support from the Bayerisches Wissenschaftsministerium and BMBF. MG received honoraria from Biogen Idec and research funding from the Landesexzellenzinitiative Hamburg. TM received honoraria from Talecris and research support from the Werner-Otto-Stiftung and Landesexzellenzinitiative Hamburg. JD received royalties from the editorial board of Up-To-Date; from Athena Diagnostics for a patent for the use of Ma2 as autoantibody test. He has received a research grant from Euroimmun, and his contribution to the current work was supported in part by grants from the National Institutes of Health and National Cancer Institute RO1CA89054, 1RC1NS068204-01, and a McKnight Neuroscience of Brain Disorders award. CG received research funding from the Deutsche Forschungs Gemeinschaft. JL received research support by the Thyssen Stiftung. RB discloses no conflicts of interest.

whole-body PET data for characteristic changes of glucose metabolism compared with controls, and the changes of this pattern during the course of the disease.

Results—Groupwise analysis revealed that patients with NMDAR-ab encephalitis showed relative frontal and temporal glucose hypermetabolism associated with occipital hypometabolism. Cross-sectional analysis of the group demonstrated that the extent of these changes is positively associated with clinical disease severity. Longitudinal analysis of two cases showed normalisation of the pattern of cerebral glucose metabolism with recovery.

Conclusions—A characteristic change in cerebral glucose metabolism during NMDAR-ab encephalitis is an increased frontotemporal-to-occipital gradient. This pattern correlates with disease severity. Similar changes have been observed in psychosis induced by NMDAR antagonists. Thus, this pattern might be a consequence of impaired NMDAR function.

Background

A recently described encephalitis subtype, mostly in young women and children, and associated with good recovery and response to immunotherapy, is characterised by antibodies (abs) directed against the NR1-subunit of the N-methyl-D-aspartate receptor (NMDAR).[1] The incidence is unknown; 1% of young patients in a German intensive care unit[2] and 4% of all encephalitis syndromes in a large British multicentre study[3] were affected. Patients often present with severe memory loss, epileptic seizures, psychiatric disturbances, especially psychosis, movement disorders, hypo-ventilation and catatonic states. Cerebral MRI shows no abnormalities in half the patients, and only unspecific changes in the grey and white matter in the remaining patients.[1] In some patients, ovarian teratomas, and seldom other tumours, are detected as the underlying cause of the disease.[1]

Single-case reports have shown temporal and extratemporal glucose hypermetabolisms in 18F-fluoro-2-deoxy-D-glucose (FDG) positron emission tomography (PET).[4–9] However, a metabolic pattern typical for NMDAR-ab encephalitis has not been described.

In order to detect underlying gonadal or extra-gonadal neoplasms, whole-body FDG-PET is frequently performed in patients with NMDAR-ab encephalitis. The objective of this study was to determine if there is a frequent or characteristic pattern of cerebral glucose metabolism in NMDAR-ab encephalitis by systematic analysis of brain FDG uptake from whole-body FDG-PETs in a cohort of retrospectively identified patients with this syndrome in order to improve diagnostic accuracy and gather insights into the pathophysiology of the disease.

Methods

Patient selection

Patients with NMDAR-ab encephalitis were retrospectively identified between 1 January 2007 and 31 July 2010 in the Department of Neurology, University Medical Center Hamburg-Eppendorf, or University Medical Center Regensburg. Diagnostic criteria where two or more acute or subacute evolved clinical symptoms (memory disturbances, psychiatric symptoms, epileptic seizures, reduced level of consciousness, movement disorder) plus either cerebrospinal fluid pleocytosis or oligoclonal immunoglobulin G (IgG) plus IgG NMDAR-ab in serum, or cerebrospinal fluid of at least 1:10. NMDAR-ab detection was performed by indirect immunofluorescence with HEK293 cells recombinantly expressing NR1 NMDAR (Mosaik Biochip, Euroimmun, Germany).[10] Data extracted from the files included basic demographics, onset of symptoms, initial hospitalisation, clinical presentation, treatment, imaging studies and disability according to the modified Rankin Scale (mRS).[11] Of 10 patients diagnosed with NMDAR-ab encephalitis between 2007 and

2010, 6 patients (4 women and 2 men, mean 21 years, range 19–39 years) had been examined by whole-body FDG-PET, two of whom had a follow-up whole-body FDG-PET. In all scans, brain FDG uptake could be extracted from the whole-body FDG-PET. In all cases, mRS was documented in patient files upon admission and at last follow-up visit. All patients were suffering from moderate to severe disease (median mRS 4.5, range 3–5). Further demographic data is provided in the online supplementary table 1. All patients had detectable serum NMDAR-abs and presented with prominent psychiatric features. In all patients included, cerebral MRI with axial FLAIR, diffusion-weighted images, native T1 and gadolinium (gd)-enhanced T1 images were available within 2 weeks prior to FDG-PET. All patients underwent repeated neuropsychological testing (median 3 times) during the course of disease (median 8 weeks after onset). Recovery of cognitive functions correlated well with decrease of mRS (not shown).

FDG-PET

Whole-body FDG PET/CT for detection of neoplasms had been performed with a PET/CT system Gemini GXL 10 (Royal Philips Electronics, The Netherlands) or Biograph 16 (Siemens, Germany). Imaging started with a non-enhanced, low-dose CT of the whole body about 60 min after intravenous injection of 300–400MBq FDG. Whole-body PET was performed immediately after CT. Transversal PET slices were reconstructed with CT-based attenuation correction using an iterative algorithm. Spatial resolution was 9 mm full-width-at-half-maximum (FWHM). For further processing, the attenuation-corrected PET images of the brain were separated from the whole-body scan using the PMOD software package V. 3.204 (PMOD Technologies, Zurich, Switzerland).

Voxel-based statistical testing

The brain image was stereotactically normalised using the ‘Normalize-Tool’ of the Statistical Parametric Mapping software package (SPM2, default parameter settings).[12] The stereotactically normalised image was smoothed with an isotropic 3D Gaussian kernel with 14 mm FWHM. The confounding effect of global FDG uptake was removed by scaling voxel intensities in the smoothed image to the average voxel intensity over the whole brain (SPM proportional scaling).

For single-subject analysis, the scaled FDG-PET brain image of the patient was compared voxel-by-voxel with corresponding images of a control group described below (one-sided two sample t tests for hypo- and hypermetabolism; α=0.001 uncorrected for multiple comparisons, no non-sphericity correction). Only effects in clusters of at least 1 ml were considered. Mean FDG uptake in the frontal, temporal and occipital lobe was calculated by using volumes of interest predefined in the TD Lobes atlas of the WFU Pick Atlas Toolbox V.2.4).[13] The ratio of frontal-to-occipital and temporal-to-occipital FDG uptake was tested for correlation with the mRS using the Spearman test, and for groupwise comparison (mRS>0 to controls) by unpaired two-tailed t test.

For detection of changes in the follow-up PET compared with the baseline PET, voxel-based subtraction analysis was performed as previously described.[14] Images were smoothed with an isotropic 3D Gaussian kernel with 30 mm FWHM prior to subtraction analysis. Effects larger than 2 SDs were considered statistically significant.

For group analysis, scaled FDG uptake was compared voxel-by-voxel between the group of patients and the control group. One patient (patient #6) was excluded from the group analysis, because of the limited field of view (online supplementary figure 1). Statistical significance was defined via a false discovery rate of 0.05.[15]

The control group consisted of 24 patients who underwent whole-body FDG-PET, including the brain, because of non-CNS oncological indications: gonadal tumour (n=5), bronchial (n=3), thyroid (n=1), oesophageal (n=1), pancreatic (n=1) or mamma (n=1) carcinoma, non-Hodgkin's (n=4) or Hodgkin's (n=2) lymphoma, melanoma (n=3), osteosarcoma (n=1), rhabdomyosarcoma (n=1) or granulosa cell tumour (n=1) (age 38±16 years, 14 women; age not significantly different from the group with NMDAR-ab encephalitis, p=0.10, two-sided t test). Exclusion criteria were known psychiatric or neurological disorder, psychotropic medication at the time of the PET, and abnormal PET findings in the brain based on visual evaluation of the PET images by an experienced reader. The control subjects had been tested by SPM2 statistical analysis using the leave-one-out strategy. Subjects with any significant cluster of either hypo or hypermetabolism ($\alpha = 0.05$, corrected for multiple comparisons) had been excluded. PET acquisition and image reconstruction protocol was the same in the group of NMDA-ab encephalitis patients and the control group.

Results

Patient characteristics

Cerebral MRI was normal in four patients (#1,4–6). Patient #2 had multiple small subcortical T2-hyperintensities without Gd enhancement, and patient #3 had three periventricular T2-hyperintense and slightly Gd-enhancing lesions without corresponding FDG-PET abnormalities.

Median time between onset of the disease and first FDG-PET was 10 weeks (range 10 weeks prior to 30 weeks after disease onset). Patients #2–6 were at the peak of the disease. In one male patient (#1), PETwas performed 10 weeks prior to onset of symptoms to screen for extragonadal manifestations of a differentiated teratoma (left testis pT2N0M0, diagnosis 5 months before, no tumour on right-sided testis biopsy). No tumour was found in the other patients. Two patients had epileptic seizures prior to PET imaging (1, 4 weeks) and were successfully treated with anticonvulsants at the time of FDG-PET (patients #5 and #6). In the other patients, no seizures occurred before PET imaging.

First-line treatment was with steroids (median 1 week, range 4 weeks prior to 15 weeks after first PET). Five patients were additionally treated with plasmapheresis, two received intravenous Igs, four were eventually treated with rituximab and one with cyclophosphamide. Outcome at last follow-up was generally good (two patients each mRS 0, mRS 1, mRS 2), and all patients had shown improvement of varying degrees.

Individual regional abnormalities of brain glucose metabolism

Voxel-based statistical analysis of the individual cerebral FDG-PET showed abnormalities in each of the six patients (table 1, representative images in figure 1, all images available in online supplementary figure 1). While some patients displayed only restricted temporomesial or frontal increased uptake (figure 1, patient #1 and #2), in others widespread frontotemporal hyper- and bioccipital hypometabolism were observed (figure 1, patient #4 and #6). In patients with pronounced changes (figure 1, patient #4 and #6), also cerebellar cortical hypermetabolism was noticed.

One male patient (#1) did not have any symptoms at the time of FDG-PET (mRS 0), but was severely affected (mRS 5) 10 weeks later. At that time, no additional FDG-PET was performed. NMDAR positivity was diagnosed after recovery. Thus, this image represents a presymptomatic situation in which already slight temporomesial hypermetabolism was detected (figure 1, left panel). Of note, this was the only patient in whom FDG-PET only revealed mesiotemporal hypermetabolism, but neither frontal hyper- nor occipital hypometabolism.

Taken together, all patients with NMDAR-ab encephalitis with the exception of patient #3 showed temporal glucose hypermetabolism. Moreover, all but the presymptomatic patient (#1) showed either increased frontal or decreased occipital glucose metabolism.

Recovery is associated with decreased frontotemporal and increased occipital glucose metabolism

In two patients (#3 and #5, initial mRS 3 and 5, respectively), initial brain glucose metabolism during active disease could be compared with PET images after recovery (116 and 128 weeks after onset of disease, both mRS 1). In both cases, individual subtraction analysis revealed an almost identical pattern of changes in glucose metabolism upon recovery with decreased frontal and increased occipital metabolism (figure 2A). Of note, in both cases, the changes were much more widespread than expected by single-subject analysis for abnormal glucose metabolism compared with the control group (online supplementary figure 1). In summary, upon clinical recovery the intra-individual analysis showed a reverse pattern compared with the frontal and temporal hyper- and occipital hypometabolism observed in the single-subject analysis.

Group analysis confirms temporal and frontal hypermetabolism in association with occipital hypometabolism as a general pattern of abnormal brain glucose metabolism in NMDAR-ab encephalitis

FDG-PETof the presymptomatic patient and the remaining four patients with clinically active disease and full field-of-view was compared with the control group (online supplementary figure 1, patients #1–5). Statistically significant hypermetabolism was confirmed in both temporomesial areas, in the right prefrontal cortex and frontobasal areas. Significant and widespread hypo-metabolism was confirmed in bioccipital areas extending to left-sided parietal areas (figure 2B).

The fronto- and temporo-to-occipital gradient of cerebral FDG uptake correlates with disease severity and normalises after recovery

The pattern of individual abnormalities in FDG uptake, or the changes upon recovery, indicated that relative frontal and temporal hyper and occipital hypometabolism were characteristic changes in FDG-PET imaging in NMDAR-ab encephalitis in four of five patients with active disease (patients #3–6). Group analysis confirmed this pattern. However, cerebral FDG uptake in our analysis of regional hyper- and hypometabolism was normalised to individual whole-brain uptake, and does not represent absolute, but relative changes. Thus, both observations the relative frontal and temporal hypermetabolism and the relative occipital hypometabolism might result from the same mechanism, an increased gradient of frontal and temporal areas to the occipital lobes. We tested this hypothesis by calculating an individual fronto-to-occipital FDG uptake ratio (F/O-R) and temporo-to-occipital FDG uptake ratio (T/O-R) on the basis of relative FDG uptake in anatomically defined temporal, frontal and occipital lobes in the control group and the patients. In the control group, we found a slightly lower FDG uptake in the frontal and temporal lobes compared with the occipital lobes (F/O-R: mean ± SDs 0.88±0.06, range 0.75–1.0, 95% CI 0.85 to 0.90; T/O-R: mean ± SD 0.83±0.04, range 0.75–0.90, 95% CI 0.81 to 0.84). In our patients with NMDAR-ab encephalitis, both F/O-R and T/O-R in one of two PETs performed in moderate disease (mRS 3), and in all PETs performed during severe disease (mRS 4–5), were abnormally elevated (upper limit defined as mean + 2SDs of controls: F/O-R 1.0, T/O-R 0.91, figure 3A,B). The F/O-R and T/O-R in PETs taken during active disease (mRS >0) were significantly higher compared with controls (F/O-R: 1.02±0.08, unpaired two-tailed t test, p=0.001, T/O-R: 1.00±0.09, unpaired two-tailed t test, p<0.001). Moreover, the F/O-R and T/O-R in patients with NMDAR-ab encephalitis both strongly correlated with

disease severity measurement as mRS (F/O-R: Spearman correlation coefficient=0.818, p=0.024; T/O-R, Spearman correlation coefficient=0.873, p=0.01).

Next, we asked whether the F/O-R and T/O-R returned to normal values upon recovery. In both patients (patient #3, initial mRS 3, patient #5, initial mRS 5), F/O-R as well as the T/O-R were initially abnormal and decreased to normal values within mean ±2SDs of controls in the follow-up PET, when, clinically, both were only mildly affected (mRS 1, figure 3C,D).

Discussion

In this study, we analysed the brain glucose metabolism detected by FDG-PET in a cohort of patients with NMDAR-ab encephalitis. We found a pattern of abnormalities consisting of a relative hypermetabolism in the frontal and temporal lobes, and a relative hypometabolism in the occipital lobes in four of five patients during active disease. Patient #2 underwent FDG-PET imaging late after disease onset (30 weeks) and had a mainly psychiatric manifestation of the disease. Both might be the reasons for the circumscribed changes of cerebral glucose metabolism in this case. The extent of the changes of cerebral glucose metabolism was associated with clinical disability and recovery of the disease. Indeed, the ratios of frontal-to-occipital, and temporal-to-occipital FDG uptake, were reliable markers for the active disease, returned to normal upon recovery and correlated with disease severity. In addition, a restricted temporomesial hypermetabolism was detected in a patient with presymptomatic NMDAR-ab encephalitis.

Previous single-case reports have reported FDG-PET images in NMDAR-ab encephalitis. In seven patients with ovarian teratoma and encephalitis, a combination suggesting NMDAR-ab encephalitis although NMDAR-ab were not tested for, mainly uni- or bilateral temporal, in some cases cerebellar hypermetabolisms, and in one patient occipital hypometabolism had been observed.[1617] In a severe case of NMDAR-ab encephalitis, symmetric hypometabolism of the occipital lobes and cerebellum and asymmetric hypermetabolism of the frontal, temporal and parietal lobes were detected.[5] In less severe cases, only right frontolateral hypermetabolism,[7] or only occipital hypometabolism, was described.[8] These observations are in line with our findings. However, some published cases differ from this pattern. A case described striatal hypermetabolism in addition to occipital hypometabolism,[4] although the interpretation of these findings is difficult due to concurrent phenobarbital, midazolam and phenytoin medication. A study in which FDG-PET was examined in three patients mentions areas of hypermetabolism in frontotemporal, cerebellar and occipital regions, although individual images and detailed clinical information of these patients were not provided.[9] Furthermore, in two young girls (aged 3 and 7 years), predominantly unilateral temporal cortical hypometabolism without any areas of hypermetabolism were reported.[18] Since our cohort represents young adults (mean 21 years), this might be due to different abnormalities of brain glucose metabolism in children and teenagers with this disease. Similar to our observations, normalisation of FDG-PET abnormalities after recovery has been observed previously in two cases (bifrontal hypermetabolism[6]; striatal hyper and occipital hypometabolism[4]).

Abnormalities in brain FDG-PET have long been known to occur in autoimmune encephalitis of various origins. In encephalitis attributed to voltage-gated potassium channel complex antibodies (now related to Lgi1 or Caspr2 antibodies), bilateral temporomesial hypermetabolism and frontal and/or temporal hypometabolism have been described.[19–21] In paraneoplastic limbic encephalitis with classical onconeural antibodies (anti-Hu), usually only temporomesial hypermetabolism is observed.[2223] In neuropsychiatric lupus erythematosus, as NMDAR-ab encephalitis, an immune-mediated disease frequently associated with psychosis, often striatal hypermetabolism and sometimes widespread

frontoparietal hypometabolism were reported.[2425] In none of these cases, frontal hypermetabolism in combination with occipital hypometabolism, was identified. Hence, the pattern of abnormal brain glucose metabolism detected in NMDAR-ab encephalitis might be characteristic of this syndrome.

The pathophysiological basis of this metabolic signature of NMDAR-ab encephalitis is not known. However, the few available autopsy studies[2627] in NMDAR-ab encephalitis do not show extensive neuronal loss, complement deposition, or cellular infiltration, arguing against cellular or complement-mediated cytotoxicity as has been observed in other types of autoimmune encephalitis.[28] Rather, meningeal plasma cells are observed.[29] Therefore, it is tempting to speculate, that the detected cerebral glucose metabolism is caused by a potentially reversible disruption of synaptic NMDAR function by NMDAR-abs. In vitro, this has been shown by whole-cell patch clamp recordings in cultured rat hippocampal neurons as patients' antibodies specifically decreased synaptic NMDAR-mediated miniature excitatory postsynaptic currents without affecting α-amino-3-hydroxy-5-methyl-4-isoxazolepropionic acid (AMPA) receptor-mediated currents.[126] Glutamatergic signalling via NMDAR in humans is observed widely in limbic, frontal, temporal and cerebellar areas.[30] NMDAR antagonism has a 10-fold greater effect on GABAergic (γ-Aminobutyric acid (GABA)) than on glutamatergic cells. The downregulation of the GABAergic tone,[31] therefore, leads to an overall state of disinhibition with increased excitatory glutamate effects via non-NMDA glutamate receptors, especially in the frontal lobes.[32] Further evidence for this hypothesis stems from the fact, that the anaesthetic, ketamine, is an NMDAR antagonist[33] which induces dissociative anaesthesia, vivid hallucinations and frank psychosis in humans, features in part resembling symptoms of patients with NMDAR-ab encephalitis.[34] Of note, if ketamine is applied to healthy human subjects, the frontal-to-occipital gradient of glucose metabolism detected by FDG-PET is increased,[3536] a pattern that resembles the observed changes in our patients with NMDAR-ab encephalitis. In animals, similar effects were demonstrated upon treatment with ketamine and another NMDA-antagonist, phencyclidine.[3738] Taken together, we hypothesise that the pattern of abnormal brain glucose metabolism detected in NMDAR-ab encephalitis might be a direct result from disrupted NMDAR signalling.

This study has several limitations. First, the analysis was performed retrospectively, and we extracted the data of regional FDG uptake for statistical analysis from whole-body PET imaging. This resulted in reduced spatial resolution of the brain PET images compared with dedicated brain PET imaging. Second, FDG-PET was not performed in all patients diagnosed with NMDAR-ab encephalitis in our clinics, which results in a small sample size and a potential selection bias. Third, follow-up FDG-PET investigations were only available from a minority of patients.

In conclusion, the data presented provide a detailed description of changes of brain glucose metabolism in patients with NMDAR-ab encephalitis, consisting of an increased frontotemporal-to-occipital gradient, which correlates with disease severity. As some aspects of the pattern resemble changes in brain glucose metabolism in drug-induced psychosis, it is tempting to speculate that the neuropsychiatric symptoms characteristic for NMDAR-ab encephalitis are linked to changes of brain metabolism described herein. Larger prospective studies are needed to further delineate the pattern of NMDAR-ab encephalitis and reproduce these observations.

Supplementary Material

Refer to Web version on PubMed Central for supplementary material.

Acknowledgments

The authors are very grateful for support in patient treatment, data acquisition and advice by Daniel Schöttle, Nils Freundlieb, Manuel Friese, Alexander Münchau and Klaus-Peter Wandinger.

References

1. Dalmau J, Lancaster E, Martinez-Hernandez E, et al. Clinical experience and laboratory investigations in patients with anti-NMDAR encephalitis. Lancet Neurol. 2011; 10:63–74. [PubMed: 21163445]
2. Prüss H, Dalmau J, Harms L, et al. Retrospective analysis of NMDA receptor antibodies in encephalitis of unknown origin. Neurology. 2010; 75:1735–9. [PubMed: 21060097]
3. Granerod J, Ambrose HE, Davies NW, et al. UK Health Protection Agency (HPA) Aetiology of Encephalitis Study Group. Causes of encephalitis and differences in their clinical presentations in England: a multicentre, population-based prospective study. Lancet Infect Dis. 2010; 10:835–44. [PubMed: 20952256]
4. Maeder-Ingvar M, Prior JO, Irani SR, et al. FDG-PET hyperactivity in basal ganglia correlating with clinical course in anti-NDMA-R antibodies encephalitis. J Neurol Neurosurg Psychiatry. 2010; 32:235–6. [PubMed: 20667855]
5. Mohr BC, Minoshima S. F-18 fluorodeoxyglucose PET/CT findings in a case of anti-NMDA receptor encephalitis. Clin Nucl Med. 2010; 35:461–3. [PubMed: 20479604]
6. Iizuka T, Sakai F, Ide T, et al. Anti-NMDA receptor encephalitis in Japan: long-term outcome without tumor removal. Neurology. 2008; 70:504–11. [PubMed: 17898324]
7. Greiner H, Leach JL, Lee KH, et al. Anti-NMDA receptor encephalitis presenting with imaging findings and clinical features mimicking Rasmussen syndrome. Seizure. 2011; 20:266–70. [PubMed: 21146427]
8. Naeije G, de Hemptinne Q, Depondt C, et al. Acute behavioural change in a young woman evolving towards cerebellar syndrome. Clin Neurol Neurosurg. 2010; 112:509–11. [PubMed: 20347215]
9. Irani SR, Bera K, Waters P, et al. N-methyl-D-aspartate antibody encephalitis: temporal progression of clinical and paraclinical observations in a predominantly non-paraneoplastic disorder of both sexes. Brain. 2010; 133:1655–67. [PubMed: 20511282]
10. Wandinger KP, Saschenbrecker S, Stoecker W, et al. Anti-NMDA-receptor encephalitis: a severe, multistage, treatable disorder presenting with psychosis. J Neuroimmunol. 2011; 231:86–91. [PubMed: 20951441]
11. Van Swieten JC, Koudstaal PJ, Visser MC, et al. Interobserver agreement for the assessment of handicap in stroke patients. Stroke. 1988; 19:604–7. [PubMed: 3363593]
12. Friston KJ, Holmes AP, Worsley KJ, et al. Statistical Parametric Maps in Functional imaging: a General Linear Approach. Hum Brain Mapp. 1995; 2:189–210.
13. Maldjian JA, Laurienti PJ, Burdette JH. Precentral gyrus discrepancy in electronic versions of the Talairach atlas. Neuroimage. 2004; 21:450–5. [PubMed: 14741682]
14. Apostolova I, Lindenau M, Fiehler J, et al. Detection of a possible epilepsy focus in a preoperated patient by perfusion SPECT and computer-aided subtraction analysis. Nuklearmedizin. 2008; 47:N65–8. [PubMed: 18988338]
15. Rorden C, Bonilha L, Nichols TE. Rank-order versus mean based statistics for neuroimaging. Neuroimage. 2007; 35:1531–7. [PubMed: 17391987]
16. Ances BM, Vitaliani R, Taylor RA, et al. Treatment-responsive limbic encephalitis identified by neuropil antibodies: MRI and PET correlates. Brain. 2005; 128:1764–77. [PubMed: 15888538]
17. Dadparvar S, Anderson GS, Bhargava P, et al. Paraneoplastic encephalitis associated with cystic teratoma is detected by fluorodeoxyglucose positron emission tomography with negative magnetic resonance image findings. Clin Nucl Med. 2003; 28:893–6. [PubMed: 14578703]
18. Pillai SC, Gill D, Webster R, et al. Cortical hypometabolism demonstrated by PET in relapsing NMDA receptor encephalitis. Pediatr Neurol. 2010; 43:217–20. [PubMed: 20691947]

19. Fauser S, Talazko J, Wagner K, et al. FDG-PET and MRI in potassium channel antibody-associated non-paraneoplastic limbic encephalitis: correlation with clinical course and neuropsychology. Acta Neurol Scand. 2005; 111:338–43. [PubMed: 15819715]
20. Gast H, Schindler K, Z'graggen WJ, et al. Improvement of non-paraneoplastic voltage-gated potassium channel antibody-associated limbic encephalitis without immunosuppressive therapy. Epilepsy Behav. 2010; 17:555–7. [PubMed: 20163992]
21. Chatzikonstantinou A, Szabo K, Ottomeyer C, et al. Successive affection of bilateral temporomesial structures in a case of non-paraneoplastic limbic encephalitis demonstrated by serial MRI and FDG-PET. J Neurol. 2009; 256:1753–5. [PubMed: 19434439]
22. Scheid R, Lincke T, Voltz R, et al. Serial 18F-fluoro-2-deoxy-D-glucose positron emission tomography and magnetic resonance imaging of paraneoplastic limbic encephalitis. Arch Neurol. 2004; 61:1785–9. [PubMed: 15534190]
23. Basu S, Alavi A. Role of FDG-PET in the clinical management of paraneoplastic neurological syndrome: detection of the underlying malignancy and the brain PET-MRI correlates. Mol Imaging Biol. 2008; 10:131–7. [PubMed: 18297363]
24. Weiner SM, Otte A, Schumacher M. Alterations of cerebral glucose metabolism indicate progress to severe morphological brain lesions in neuropsychiatric systemic lupus erythematosus. Lupus. 2000; 9:386–9. [PubMed: 10878734]
25. Krakauer M, Law I. FDG-PET brain imaging in neuropsychiatric systemic lupus erythematosis with choreic symptoms. Clin Nucl Med. 2009; 34:122–3. [PubMed: 19352272]
26. Hughes EG, Peng X, Gleichman AJ, et al. Cellular and synaptic mechanisms of anti-NMDA receptor encephalitis. J Neurosci. 2010; 30:5866–75. [PubMed: 20427647]
27. Tüzün E, Zhou L, Baehring JM, et al. Evidence for antibody-mediated pathogenesis in anti-NMDAR encephalitis associated with ovarian teratoma. Acta Neuropathol. 2009; 118:737–43. [PubMed: 19680671]
28. Gultekin SH, Rosenfeld MR, Voltz R, et al. Paraneoplastic limbic encephalitis: neurological symptoms, immunological findings and tumour association in 50 patients. Brain. 2000; 123:1481–94. [PubMed: 10869059]
29. Martinez-Hernandez E, Horvath J, Shiloh-Malawsky Y, et al. Analysis of complement and plasma cells in the brain of patients with anti-NMDAR encephalitis. Neurology. 2011; 77:589–93. [PubMed: 21795662]
30. Stone JM. Imaging the glutamate system in humans: relevance to drug discovery for schizophrenia. Curr Pharm Des. 2009; 15:2594–602. [PubMed: 19689330]
31. Grunze HC, Rainnie DG, Hasselmo ME, et al. NMDA-dependent modulation of CA1 local circuit inhibition. J Neurosci. 1996; 16:2034–43. [PubMed: 8604048]
32. Gunduz-Bruce H. The acute effects of NMDA antagonism: from the rodent to the human brain. Brain Res Rev. 2009; 60:279–86. [PubMed: 18703087]
33. Orser BA, Pennefather PS, MacDonald JF. Multiple mechanisms of ketamine blockade of N-methyl-D-aspartate receptors. Anesthesiology. 1997; 86:903–17. [PubMed: 9105235]
34. Krystal JH, Karper LP, Seibyl JP, et al. Subanesthetic effects of the noncompetitive NMDA antagonist, ketamine, in humans. Psychotomimetic, perceptual, cognitive, and neuroendocrine responses. Arch Gen Psychiatry. 1994; 51:199–214. [PubMed: 8122957]
35. Vollenweider FX, Leenders KL, Scharfetter C, et al. Metabolic hyperfrontality and psychopathology in the ketamine model of psychosis using positron emission tomography (PET) and [18F]fluorodeoxyglucose (FDG). Eur Neuropsychopharmacol. 1997; 7:9–24. [PubMed: 9088881]
36. Vollenweider FX, Leenders KL, Oye I, et al. Differential psychopathology and patterns of cerebral glucose utilisation produced by (S)- and (R)-ketamine in healthy volunteers using positron emission tomography (PET). Eur Neuropsychopharmacol. 1997; 7:25–38. [PubMed: 9088882]
37. Hammer RP, Herkenham M, Pert CB, et al. Correlation of regional brain metabolism with receptor localization during ketamine anesthesia: combined autoradiographic 2-[3H]deoxy- D-glucose receptor binding technique. Proc Natl Acad Sci U S A. 1982; 79:3067–70. [PubMed: 6283555]
38. Weissman AD, Dam M, London ED. Alterations in local glucose utilization induced by phencyclidine. Brain Res. 1987; 435:29–40. [PubMed: 3427457]

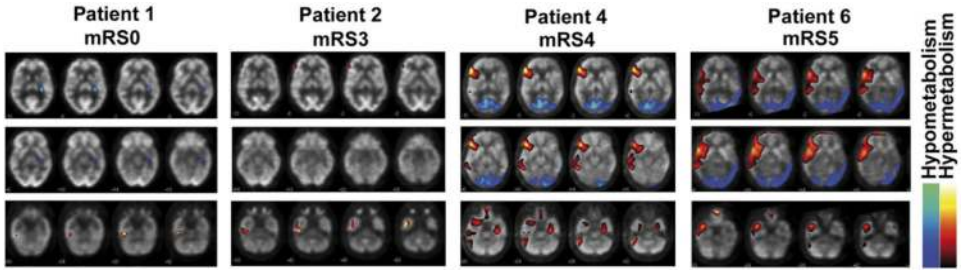

Figure 1.

Representative images of abnormal cerebral glucose metabolism in individual patients with N-methyl-D-aspartate receptor antibody encephalitis detected by 18F-fluoro-2-deoxy-d-glucose positron emission tomography. Patients with mild or moderate clinical severity (patients #1 and #2; mRS ≤3) show temporomesial hyperintensities, whereas more widespread frontal and temporal hyperintensities and occipital hypointensities in patients with severe disease (patients #4 and #6; mRS >3) are observed. Representative sections are shown (all images available in online supplementary figure 1). Significant hyper- and hypometabolism is colour/gray-scale coded as depicted in the legend. mRS, modified Rankin Scale.

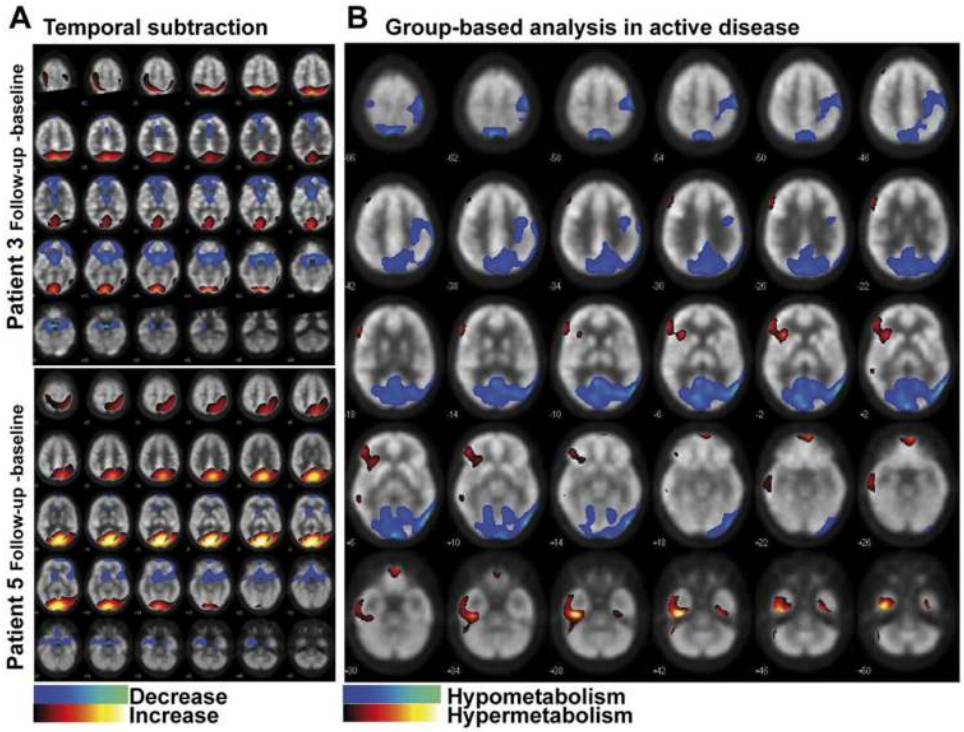

Figure 2.

Changes upon recovery and the common pattern of abnormal cerebral glucose metabolism in N-methyl-D-aspartate receptor antibodies (NMDAR-ab) encephalitis. (A) Normalisation of 18F-fluoro-2-deoxy-d-glucose positron emission tomography brain metabolism in NMDAR-ab encephalitis in two patients. Subtraction analysis for both patients (baseline vs follow-up; threshold at 2 SDs). Increase/decrease of metabolism upon recovery according to legend. (B) Groupwise analysis of patients with NMDAR-ab encephalitis during active or presymptomatic disease (n=5) compared with controls (n=24; false detection rate<0.05). Significant temporal, frontobasal, cerebellar and right-sided frontal hypermetabolism is detected, as well as occipital and asymmetric parietal hypometabolism.

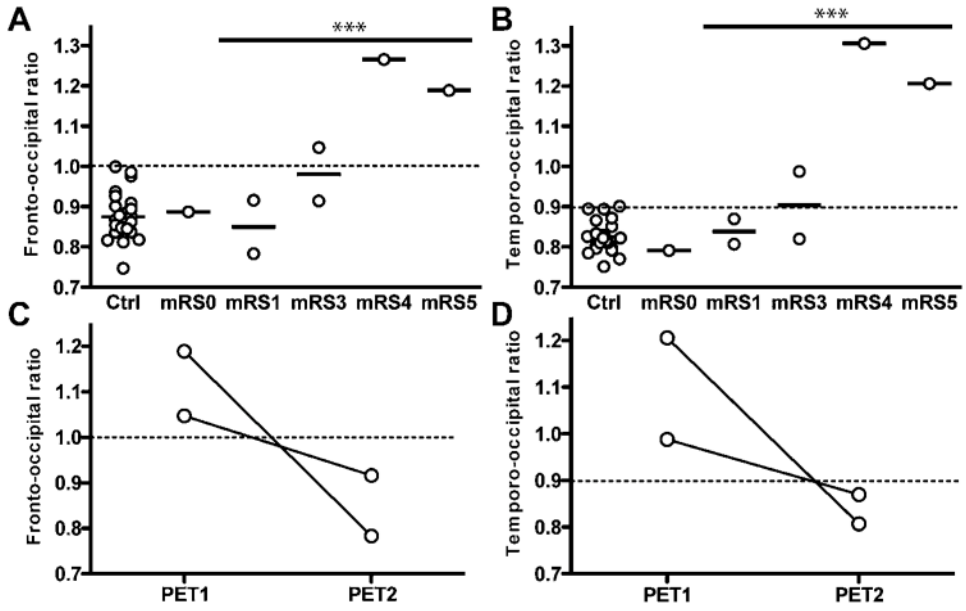

Figure 3.

An increased frontal- and temporal-to-occipital 18F-fluoro-2-deoxy-d-glucose (FDG) uptake is associated with disease severity in N-methyl-D-aspartate receptor antibodies encephalitis. Ratio of mean frontal to mean occipital (A), and of mean temporal to mean occipital FDG uptake (B), in controls and patients by disease severity modified Rankin Scale (mRS). Both ratios are significantly elevated in active disease (mRS >0) compared with controls (unpaired two-tailed t test, $p<0.001$). (C/D) Normalisation of fronto-occipital and temporo-occipital ratio upon clinical recovery in two individual patients. The upper limit defined as mean ± 2SDs of the control group is depicted as dotted line.

Table 1

18F-fluoro-2-deoxy-d-glucose positron emission tomography (FDG-PET) characteristics in patients with N-methyl-D-aspartate receptor antibody encephalitis

PET characteristics	Number of patients	Patient#
Abnormalities	6/6	1–6
Hypermetabolism		
Unilateral temporal	4/6	1, 2, 5
Bilateral temporal	2/6	4, 6
Cerebellar	3/6	4, 5, 6
Frontolateral	3/6	2, 4, 6
Frontobasal	3/6	2, 3, 6
Hypometabolism		
Bioccipital	3/6	4, 5, 6